Statistical Cross-Linking at the Si(111)/SiO_2 Interface

D.-A. Luh, T. Miller, and T.-C. Chiang*

Department of Physics, University of Illinois at Urbana-Champaign, 1110 West Green Street, Urbana, Illinois 61801-3080
and Seitz Materials Research Laboratory, University of Illinois at Urbana-Champaign,
104 South Goodwin Avenue, Urbana, Illinois 61801-2902

(Received 7 February 1997)

Angle-resolved photoemission measurements of the Si $2p$ core level as a function of polar emission angle were carried out to investigate the atomic populations and depth distributions of Si in various oxidation states for a SiO_2 film thermally grown on Si(111). The suboxide states including Si^{1+}, Si^{2+}, and Si^{3+} exhibit different depth distributions. Despite these differences, the results are consistent with a chemically abrupt interface. A simple model based on the statistical cross-linking of dangling bonds between a bulk-truncated Si and an amorphous SiO_2 layer explains our observations. [S0031-9007(97)04292-0]

PACS numbers: 68.35.Bs, 79.60.Jv

The structure of the Si/SiO_2 interface is a subject of considerable interest [1–9], and yet a detailed understanding has been lacking because of the amorphous nature of the SiO_2 film which renders traditional diffraction techniques inapplicable or inadequate. There has been considerable debate in the literature regarding the chemical profile of this interface. The simplest model for this structure is that obtained by joining a bulk-truncated Si lattice to pure SiO_2, with all of the dangling bonds from both sides stitched together. This concept of bond stitching is motivated by the fact that there are few electrical defects at the interface, and therefore few dangling bonds are expected. The result is an abrupt interface, but still, Si suboxide must exist at the interface because of the cross-link between Si and SiO_2. While this simple model is intuitive and appealing, some earlier studies [1,3] have suggested a graded interface involving suboxides SiO_x ($0 < x < 2$) extending up to 10 Å into the oxide layer.

Of all experimental techniques, the most direct probe of the interface chemical structure is photoemission [1–8]. High-resolution spectra of the Si $2p$ core level show five components, of which one corresponds to Si in the bulk bonding environment and the other four correspond to Si in various oxidation states (Si^{1+}, Si^{2+}, Si^{3+}, and Si^{4+}) [1–8,10]. In the present study, we employ angle-resolved photoemission to examine the intensities of these individual components as a function of the polar emission angle. These intensities are related to the atomic populations of the different chemical states. As the polar angle increases, the vertical probing depth becomes shorter, and the measured intensity variations provide information about the depth distribution. Our results will show that the abrupt-interface model mentioned above, augmented by a simple concept of statistical cross-linking at the interface, provides a quantitative description of the Si(111)/SiO_2 system. An explanation will be offered in regard to earlier photoemission measurements that arrived at a different conclusion.

Our photoemission measurements were carried out at the Synchrotron Radiation Center (Stoughton, Wisconsin) using the 1-GeV storage ring Aladdin. Substrates of Si(111) were prepared by outgassing at 500 °C for many hours, and then heated to 1250 °C for a few seconds to yield the clean (7×7) reconstruction. Thin oxide films were grown *in situ* by exposing the Si(111)-(7×7) substrates, held at 600 °C, to pure O_2 at 5×10^{-8} torr for 2000 s for a total exposure of 100 langmuirs. This resulted in an oxide film of about 5 Å thickness [3]. Photoemission spectra were taken with a hemispherical analyzer with an angular acceptance cone of $\pm 1.5°$. The polar emission angle θ was varied by moving the analyzer in a plane containing the $[\bar{1}2\bar{1}]$ direction of the Si substrate.

Figure 1 shows two photoemission spectra, one for $\theta = 0$ and the other for $\theta = 50°$. As shown in previous work, the spectral line shape consists of five components. The decomposition of the line shape is indicated in the figure, and the five components are labeled bulk and $S1$–$S4$ (for Si^{1+}–Si^{4+}). These five components have identical line shapes except that the Gaussian width increases progressively for higher oxidation numbers due to an increased local disorder in going from pure Si to amorphous SiO_2. The two spectra in Fig. 1 are normalized to have the same bulk peak intensity, and the oxide peak $S4$ and the suboxide peaks $S1$–$S3$ are more intense for the $\theta = 50°$ case due to a shorter vertical probing depth. All of the suboxide peaks are known to be spatially confined near the interface, since experiments on thicker films showed the intensities of $S1$–$S3$ to diminish relative to $S4$ [3].

The intensity ratios for the $S1$–$S4$ components to the bulk component are shown in Fig. 2 as a function of the polar emission angle. As the polar angle increases, all of the four ratios increase, but generally at different rates. While the increases for $S1$ and $S2$ are similar, $S3$ shows a greater rate of increase, and $S4$ shows an even greater rate. This largest rate of increase for $S4$ is understandable because $S4$ corresponds to Si in the SiO_2 film, which is

 0031-9007/97/79(16)/3014(4)$10.00

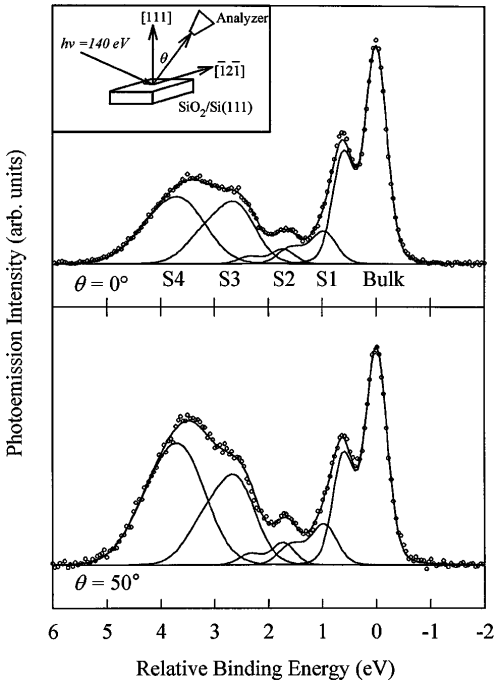

FIG. 1. Si $2p$ core-level spectra taken from $Si(111)/SiO_2$ for two different polar emission angles 0° and 50°. The circles are data points and the curves are fits. Also shown is the decomposition of the spectra into five components (bulk and $S1-S4$). The photon energy used was 140 eV. The kinetic energy of the $2p_{3/2}$ peak of the bulk component is 35.7 eV; the corresponding kinetic energy for each successive oxidation state is lower by about 0.9 eV.

closest to the surface. The differences between $S3$ and $S1/S2$ suggests that the depth distribution for Si^{3+} is significantly different from that for Si^{1+} and Si^{2+}. At first sight, one might be tempted to interpret this result as a sign of a nonabrupt, graded interface, but this is actually not so as we will discuss below.

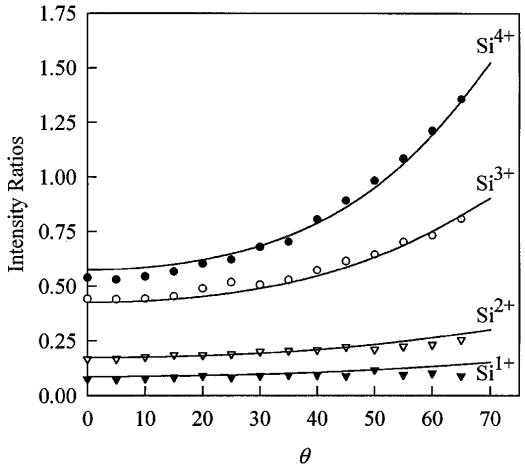

FIG. 2. Intensity ratios between the $S1-S4$ components and the bulk component as a function of the polar emission angle. The symbols represent data points, and the curves are fits to the data.

To explain the results shown in Fig. 2, we will now compute the expected intensity variations based on the abrupt-interface model. Figure 3(a) is a side view along $[11\bar{2}]$ of the Si(111) lattice, which consists of bilayers. Figures 3(b) and 3(c) show all of the possible local bonding configurations for a terminating Si atom at the interface. In each of the six cases, the four nearest neighbors of a terminating Si atom are shown. Again, we assume that the interface is formed by joining all of the dangling bonds of a bulk truncated Si(111) to SiO_2, and the dashed lines in Fig. 3 indicate the interface plane. Below this interface plane is pure Si, and there are two ways of terminating the Si(111) lattice: (1) intrabilayer termination as shown in Fig. 3(b), in which each top Si atom has one back bond and three dangling bonds protruding to the other side of the interface, and (2) interbilayer termination as shown in Fig. 3(c), in which each top Si atom has three back bonds and one dangling bond protruding to the other side of the interface. As the oxidation of the Si lattice proceeds layer by layer, the termination of the Si lattice alternates between these two cases [11]. Since thermal oxidation is a relatively local and random process resulting in uncorrelated oxidation at different parts of the surface, the two terminations are equally probable by statistics.

Above the interface plane in Figs. 3(b) and 3(c) is SiO_2, and its dangling bonds are cross-linked to the

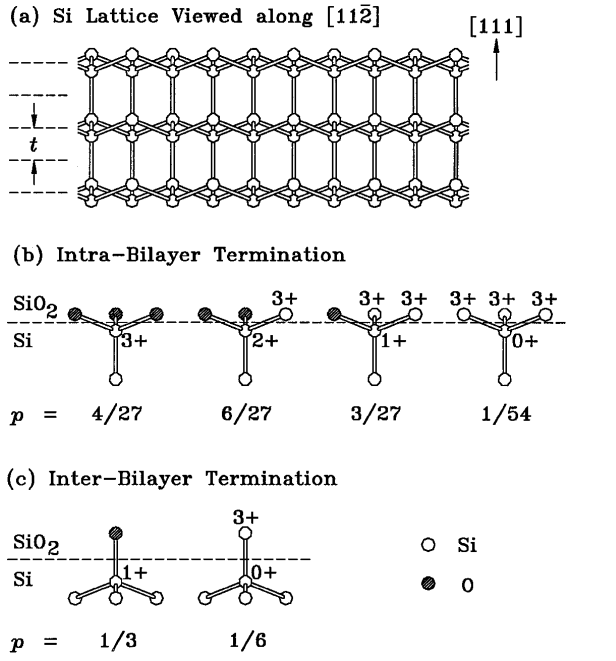

FIG. 3. (a) A model of the Si(111) lattice viewed from the side along $[11\bar{2}]$. (b) All of the possible local bonding configurations for a Si atom terminated within a bilayer (intrabilayer termination). The probabilities (p) for the four configurations are shown. (c) All of the possible local bonding configurations for a Si atom terminated in-between bilayers (interbilayer termination). The probabilities (p) for the two configurations are shown.

dangling bonds of the Si substrate. Both Si and O can be the terminating species of SiO_2. Since the film is amorphous, there should be statistically twice the number of oxygen atoms than Si atoms terminating the SiO_2. Each terminating oxygen atom will have one dangling bond, and each terminating Si could have up to three dangling bonds. However, the oxidation occurs at high temperatures, and a local minimization of free energy makes multiple dangling bonds on a terminating Si very unlikely [12]. Thus, our model is for single dangling bonds from both Si and O, with a $1:2$ population ratio between the two kinds. Taking into account the symmetry-equivalent degeneracies, the probability p for each of the configurations shown in Figs. 3(b) and 3(c) can be calculated, and the results are indicated in the figure [13]. Note that each Si atom just above the interface plane has three other bonds connected to oxygen atoms in the SiO_2 film (not shown). A straightforward counting of the oxygen neighbors yields the assignments of oxidation numbers as shown in Fig. 3. It is interesting to observe that Si^{1+} and Si^{2+} are confined to the atomic layer just below the interface boundary, while Si^{3+} can be on either side of this boundary. This explains qualitatively why the behavior of $S3$ in Fig. 2 is different from that of $S1$ and $S2$.

The calculation of the intensities involves the probabilities mentioned above and an exponential weighting factor $\exp[-D/(\lambda\cos\phi)]$, where D is the thickness of the material above the emitting species, λ is the electron mean free path ($\sim$5 Å; this may be slightly different between Si and SiO_2, but this difference is ignored), and ϕ is the polar angle of emission within the crystal. Because of surface refraction, the internal angle ϕ and the external angle θ are not the same, and are related by [14]

$$\sin\phi = \sqrt{\frac{E_k}{E_k + V_0}}\,\sin\theta\,,$$

where V_0 is the inner potential ($\sim$15 eV), and E_k is the kinetic energy of the photoelectron in vacuum. The above model yields an attenuation factor $\exp[-t/(\lambda\cos\phi)]$ for each atomic layer, where $t = 1.57$ Å is the atomic layer thickness illustrated in Fig. 3(a). Thus, the attenuation for the layer of atoms just below the interface plane involves a distance $D = T$, where T($\sim$5 Å) is the thickness of the oxide layer, while $D = T - t$ for the layer of atoms just above the interface plane. The calculation is straightforward, and the resulting equations, apart from an overall proportional constant, are

$$I_{4+} = n_{4+}\left[1 - \exp\left(-\frac{T-t}{\lambda\cos\phi}\right)\right]\lambda\cos\phi\,,$$

$$I_{3+} = n_{\mathrm{Si}}\left[\frac{4}{27} + \frac{2}{3}\exp\left(\frac{t}{\lambda\cos\phi}\right)\right]\exp\left(-\frac{T}{\lambda\cos\phi}\right),$$

$$I_{2+} = n_{\mathrm{Si}}\frac{2}{9}\exp\left(-\frac{T}{\lambda\cos\phi}\right),$$

$$I_{1+} = n_{\mathrm{Si}}\frac{4}{9}\exp\left(-\frac{T}{\lambda\cos\phi}\right),$$

$$I_B = \frac{n_{\mathrm{Si}}[\frac{22}{27} + \frac{5}{27}\exp(\frac{t}{\lambda\cos\phi})]}{\exp(\frac{t}{\lambda\cos\phi}) - 1}\exp\left(-\frac{T}{\lambda\cos\phi}\right),$$

where $n_{4+} = 2.28\times10^{22}$ cm^{-3} is the concentration of Si in SiO_2, and $n_{\mathrm{Si}} = 7.83\times10^{14}$ cm^{-2} is the number of Si atoms in an atomic layer. All physical quantities are known except V_0, T, and λ, for which we only know the values to within about $\pm20\%$.

Using the nominal values of V_0, T, and λ mentioned above, these equations yield results in fairly good agreement with the experiment. The curves shown in Fig. 2 are, however, obtained by a least squares fitting procedure with V_0, T, and λ treated as fitting parameters. The final values from the fit are $V_0 = 15.3$ eV, $T = 4.2$ Å, and $\lambda = 4.4$ Å, which are all well within the expected ranges for these quantities. It is important to note that the four curves in Fig. 2 represent intensity ratios involving no arbitrary scale factors. The good agreement means that the relative abundances of the different suboxide species are very well described by the model; this is satisfying because the argument used in our model is entirely statistical. The rates of increase as a function of θ for the different oxidation numbers are also very well reproduced by the model. In particular, the faster increase of $S3$ relative to $S1$ and $S2$ can be related to the two-layer distribution of Si^{3+} mentioned above.

It is quite remarkable that such a simple model describes the experimental results well for a system that appears complicated in many ways and has defied numerous attempts for a quantitative analysis. On the other hand, this model is very reasonable based on our general understanding of surface chemistry. An important remaining question is why some previous photoemission studies arrived at a conclusion of a nonabrupt interface. Part of the discrepancy may be semantic in nature, but there are two fundamental issues that make a significant difference: (1) In joining Si to SiO_2 to form an interface, the dangling bonds from Si can join both Si and O on the side of the SiO_2. Some previous studies assumed that only the O atoms in SiO_2 are available for bonding. A consequence of this constraint is that no Si^{2+} is present at the abrupt interface (see Fig. 3), and the presence of Si^{2+} as observed by experiment was taken to be evidence for a graded, extended suboxide SiO_x region. This assumption is unjustified and leads to incorrect relative abundances for the suboxide species. (2) In previous studies, the depth information was often inferred from a dependence of the photoelectron mean free path on the photoelectron kinetic energy, which was varied by changing the exciting photon energy. However, this type of measurement relying on the energy dependence can be significantly affected by photoelectron diffraction effects. Even for an amorphous layer, near edge and extended fine structure modulations can be important [15]. In contrast, the present experiment

relies on the angular dependence of the emission intensity, for which diffraction modulations are mostly scrambled by the amorphous SiO_2 overlayer [16].

To summarize, we presented a model for $Si(111)/SiO_2$ based on the concept of statistical cross-linking. The essence of this model is an abrupt transition from Si to SiO_2, with the dangling bonds from the two sides of the interface plane stitched together. Suboxide species including Si^{1+}, Si^{2+}, and Si^{3+} are necessarily present in the boundary layers due to the cross-linking. The amorphous nature of the SiO_2 film allows us to make a statistical analysis of the population of each species. An angle-resolved photoemission measurement was carried out to determine the abundances and depth distributions of the various oxidation states of Si, and the results are well described by the model. This work demonstrates that statistical cross-linking is a useful concept for interfaces involving amorphous/glassy materials. For the case of $Si(111)/SiO_2$, it provides a quantitative description of the chemical structure of the interface.

This material is based upon work supported by the Division of Materials Sciences, Office of Basic Energy Sciences, Department of Energy, under Grant No. DEFG02-91ER45439. Acknowledgment is also made to the Donors of the Petroleum Research Fund, administered by the American Chemical Society, and to the National Science Foundation (Grants No. DMR-95-31809 and No. DMR-95-31582) for partial support of the synchrotron beamline operation and personnel. The Synchrotron Radiation Center of the University of Wisconsin is supported by the National Science Foundation under Grant No. DMR-95-31009.

*Electronic address: t-chiang@uiuc.edu

[1] P. J. Grunthaner, M. H. Hecht, F. J. Grunthaner, and N. M. Johnson, J. Appl. Phys. **61**, 629 (1987); F. J. Grunthaner and P. J. Grunthaner, Mat. Sci. Rep. **1**, 65 (1986).

[2] G. Hollinger and F. J. Himpsel, J. Vac. Sci. Technol. A **1**, 640 (1983); Phys. Rev. B **28**, 3651 (1983); Appl. Phys. Lett. **44**, 93 (1984).

[3] F. J. Himpsel, F. R. McFeely, A. Taleb-Ibrahimi, J. A. Yarmoff, and G. Hollinger, Phys. Rev. B **38**, 6084 (1988).

[4] S. Iwata and A. Ishizaka, J. Appl. Phys. **79**, 6653 (1996); A. Ishizaka and S. Iwata, Appl. Phys. Lett. **36**, 71 (1980).

[5] J. M. Hill, D. G. Royce, C. S. Fadley, L. F. Wagner, and F. J. Grunthaner, Chem. Phys. Lett. **44**, 225 (1976).

[6] J. Finster, D. Schulze, F. Bechstedt, and A. Meisel, Surf. Sci. **152**, 1063 (1985).

[7] M. T. Sieger, D. A. Luh, T. Miller, and T.-C. Chiang, Phys. Rev. Lett. **77**, 2758 (1996).

[8] T. Hattori and T. Suzuki, Appl. Phys. Lett. **43**, 470 (1983).

[9] A. Munkholm, S. Brennan, F. Comin, and L. Ortega, Phys. Rev. Lett. **75**, 4254 (1995).

[10] M. M. B. Holl and F. R. McFeely, Phys. Rev. Lett. **71**, 2441 (1993); K. Z. Zhang, M. M. Banaszak Holl, J. E. Bender IV, S. Lee, and F. R. McFeely, Phys. Rev. B **54**, 7686 (1996); F. R. McFeely, K. Z. Zhang, M. M. Banaszak Holl, S. Lee, and J. E. Bender IV, J. Vac. Sci. Technol. B **14**, 2824 (1996). These authors performed a detailed study of spherosiloxanes and proposed a different interpretation for the chemical shifts. But their interpretation was not supported by a first-principles calculation [A. Pasquarello, M. S. Hybertsen, and R. Car, Phys. Rev. Lett. **74**, 1024 (1995)]

[11] F. M. Ross and J. M. Gibson, Phys. Rev. Lett. **68**, 1782 (1992).

[12] This problem can be viewed from a different angle. Assuming that there is a boundary Si atom in SiO_2 that is triply bonded to the Si substrate, it would be natural to consider this Si atom to be part of the Si substrate lattice. Boundary Si atoms doubly bonded to the Si substrate are incompatible with the (111) geometry on a flat terrace.

[13] Consider the intrabilayer case in Fig. 3(b). The four configurations from left to right have symmetry degeneracies of 1, 3, 3, and 1, respectively, where the factor of 3 corresponds to the three different ways to pick the special bond. Each bond to oxygen is twice as likely as to a Si bond, and thus the population factors are 2^3, 2^2, 2^1, and 2^0 for the same four configurations. Multiplying the two sets of numbers yields 8, 12, 6, and 1, which are proportional to the probabilities. The probabilities shown in Fig. 3(b) are obtained after normalization under the condition that the total probability for the four configurations is $\frac{1}{2}$. The interbilayer case can be worked out similarly.

[14] T. Miller, A. P. Shapiro, and T.-C. Chiang, Phys. Rev. B **31**, 7915 (1985).

[15] P. S. Mangat, K. M. Choudhary, D. Kilday, and G. Margaritondo, Phys. Rev. B **44**, 6284 (1991); P. S. Mangat, P. Soukiassian, K. M. Schirm, L. Spiess, S. P. Tang, A. J. Freeman, Z. Hurych, and B. Delley, Phys. Rev. B **47**, 16 311 (1993); J. A. Carlisle, M. T. Sieger, T. Miller, and T.-C. Chiang, Phys. Rev. Lett. **71**, 2955 (1993).

[16] Diffraction modulation is on the order of 10% for a crystalline system (see Ref. [14]). For the present case, this should be much less. The slight modulations that fluctuate around the model curves in Fig. 2 could be attributed to residual diffraction effects.